Published by :
http://www.ijert.org

International Journal of Engineering Research & Technology (IJERT)
ISSN: 2278-0181
Vol. 9 Issue 10, October-2020

Detection of Alzheimer's Disease on Brain MRI using Inception V3 Network

Shanmuga Skandh Vinayak E
Department of Information Technology
Siva Subramaniya Nadar College of Engineering
Chennai, India

Shahina A
Department of Information Technology
Siva Subramaniya Nadar College of Engineering
Chennai, India

Nayeemulla Khan A
School of Computing Sciences and Engineering
Vellore Institute of Technology, Chennai
Chennai, India

***Abstract*—Magnetic Resonance Imaging (MRI) has been a significant influence in the medical industry, since its early inception in the year 1977. It has enabled practitioners to better understand the organizational structure of internal organs, including that of the human brain. In this article, the MRI data of the brain is subjected to experimental tests in the process of identifying cognitive impairment such as Alzheimer's disease, using machine learning algorithms. An automatic detection system, using the deep learning network Inception V3, is proposed for this purpose. This system utilizes the edge detection algorithm in providing efficient results. The system performs with an accuracy of 82.89%, while being able to classify the images with an efficient time duration of 0.11s/sample.**

Index Terms*—*Alzheimer's disease, detection, edge, Inception V3, MRI, ADNI, Bilateral Filter, Normalization.

I. INTRODUCTION

Alzheimer's disease – A critical ramification of the cognitive function of the human brain, caused by complex brain changes and cell damage, causes dementia, and affects approximately 30 million people around the world. Amongst the most common dementia cases, the patients suffer from perturbing memory and the normal functionality of the brain. Dementia affects over 50 million individuals worldwide according to Statista [1] (figure 1) and predicted to accrue to approximately 152 million, by the year 2050. Alzheimer's disease ranks as the 2nd most severe neurological disorder in the world, with approximately 60% to 80% of the cases affected with Alzheimer's disease, develop dementia symptoms.

One of the most common and preliminary Alzheimer's disease detection tests, along with psychological examinations, is the brain MRI scanning and analysis. The medical professionals examine the MRI scans and assess possible factors that have the potential to reveal the

presence of Alzheimer's disease, such as, brain matter degeneration, tumor, etc. Although manual examinations of MRI data prove to be effective in detecting the presence of Alzheimer's disease, this process tends to reduce the efficiency of expeditious arrival of conclusions. This paper proposes an automatic detection of Alzheimer's disease from brain MRI scanned images, to improve the efficiency, in terms of accuracy and speed. This paper is organized as follows. Section II reviews the contemporary studies carried out on the detection of Alzheimer's disease. The Experimental setup and results are discussed in Section III. The limitation of this work, along with further directions are discussed in Section IV.

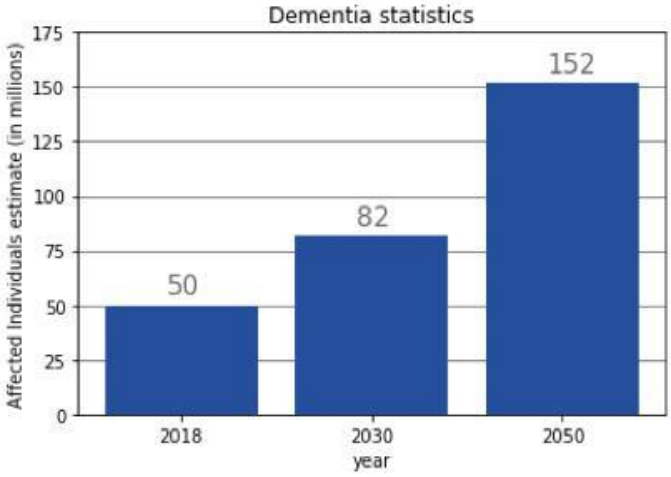

Fig. 1. Dementia disease statistics

II. RELATED WORKS ON ALZHEIMER'S DISEASE DETECTION

Reju John et al., focus on the detection of Alzheimer's disease using fractal edge detection method [11], in their work. Utilizing filtering techniques such as Sobel and Prewitt filter, they improve the edge detection mechanism and accuracy in their work. Their work adopts the methodology of classifying the MRI images based on the variation in the hippocampal mass of the brain. i.e. the gray and the white matter. Using fuzzy logic, the brain matter differences are classified as either existence of Alzheimer's disease, or as a possibility for the Alzheimer's disease to occur, or as a healthy brain.

International Journal of Engineering Research & Technology (IJERT)
ISSN: 2278-0181
Vol. 9 Issue 10, October-2020

D.P. Devanand et al., have performed a study on evaluating local deformations of the hippocampus, para hippocampal gyrus, and entorhinal cortex, in predicting conversion from mild cognitive impairment to having Alzheimer's disease [12], using MRI surface morphometry mapping. Their work follows baseline brain MRI with surface morphological analysis for patients at a single site of study. ANOVA, ANCOVA, and chi-square tests were used to compare the demographic, clinical, and MRI variables of patients (converters, non-converters to AD) and controls. Volumetric and surface morphometry of the hippocampal region for 134 patients are considered for classification, using the above methods.

Andrea Chincarini et al., in their work on local MRI analysis for the diagnosis of early and prodromal Alzheimer's disease [13], have performed experiments in detecting the presence of Alzheimer's disease conversion probabilities. This is done by studying the features present in the volume of interest, selected from the hippocampal region of the brain. The T1-weighted MRI data, obtained from Alzheimer's Disease Neuroimaging Initiative (ADNI), were subjected to analysis for obtaining the volumes of interest, by sectioning the MRI data into several slices and testing the section that provided the maximum features, before analysis. These sections were subjected to further analysis using the Random Forest algorithm, which provided the regions showing relevant features. These features were filtered and statistical models were generated using Support Vector Machine, that provided with an accuracy of AUC – 97% (sensitivity ≈ 89% at specificity ≈ 94%) for Controls from AD and Controls from MCI – converters with an AUC – 92% (sensitivity ≈ 89% at specificity ≈ 80%). MCI – converters are separated from MCI – non-converters with AUC – 74% (sensitivity ≈ 72% at specificity ≈ 65%) for a 20-fold validation.

Elaheh Moradi et al., used the concept of Low-Density Separation (LDS) in the development of a machine learning framework for early MRI-based Alzheimer's conversion prediction, in MCI subjects [14]. In this method, the images obtained from the ANDI baseline T1-weighted MP-RAGE sequence, using 1.5 T scanners, are subjected to the LDS method. The model is trained with supervised and unsupervised data simultaneously. The unsupervised data serves as a fine tuner for the machine, to identify the Alzheimer's disease location in the brain MRI using elasticnet, with the highest accuracy in discriminating Alzheimer's disease and Normal Cognition subjects. The features obtained from the LSD framework are applied to a Random Forest framework, to classify the patients with a higher risk of conversion from mild cognitive impairment to having Alzheimer's disease and the patients that have a lesser chance of such a case.

III. EXPERIMENT AND RESULTS

In this paper, a system that utilizes the edge detection technique to identify the presence of Alzheimer's disease is proposed. The experiment is conducted on an image dataset of MRI scans, to classify them based on the presence of Alzheimer's disease (AD), Mild Cognitive Impairment (MCI) and normal cognition (CN). This experiment utilizes the edge detection methodology, to detect and classify the presence of AD and signs of MCI.

A. Dataset

All the data are collected from the ADNI database [4]. The database comprises of research from 63 sites, in the regions of the United States and Canada. The multisite corporation enrolls subjects from the age of 55 to 91, recruited in over 57 sites of their operation, to produce MRI and Positron Emission Tomography (PET) scans, to study the causes and detection of AD in subjects. The data under study, obtained for this experiment, were acquired using the ADNI1 1.5T Siemens MRI scanners, with T1-weighted (recovery of magnetization before measuring the MR signal, by changing the repetition time (TR)) and dual-echo T2-weighted (decay of magnetization before measuring the MR signal, by changing the echo time (TE)) sequences. The data obtained as NIfTI files and are converted to images of coronal cross-sections. All the images are Gradwarp corrected, to redress the gradient induced spatial distortions of the MRI and B1 non-uniformity corrected, that rectifies the intensity non-uniformity error caused by the sensitivity of linearly polarized radio-frequency (RF) MRI coils, performed by ADNI. For selected images, N3 sharpening [5] is performed by ADNI, to correct the shading artifacts in the MRI, caused by intensity non-uniformity. Figures 2a and 2b, show the Gradwarp correction variation between the uncorrected and corrected images, obtained from the research work [6]. Figures 3a and 3b, show the B1 non-uniformity correction between the uncorrected and corrected images, obtained from the research work [7].

B. Edge Detection System

The edge detection is an image processing technique, that analyses an image and detects the boundaries of the objects discovered in the image [2]. The system detects for variation and discontinuities in the brightness of neighboring pixels, to arrive at a significant boundary separation.

International Journal of Engineering Research & Technology (IJERT)
ISSN: 2278-0181
Vol. 9 Issue 10, October-2020

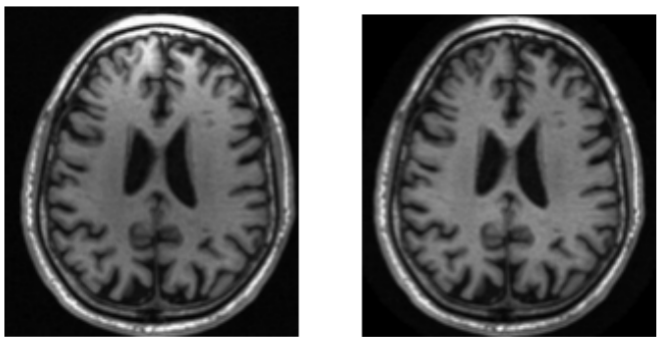

(a) Original MRI (b) Gradwarp corrected MRI

Fig. 2. Comparison between original and Gradwarp corrected MRI

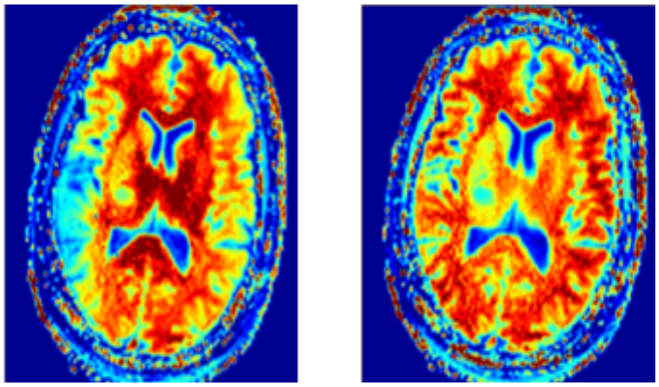

(a) Original MRI (b) B_1 corrected MRI

Fig. 3. Comparison between original and B1 corrected MRI

amongst objects in the images, which the system can utilize to classify the objects using image identification algorithms. The proposed model utilizes the classification weights of Inception V3 [3]. Inception V3 is the version 3 of Inception, an image identification neural network architecture, that has been trained using the ImageNet, to identify a range of real-world objects in existence. This trained model is utilized and the weights are updated using the training data of this experiment, to identify the three-group classification of this study during the learning process of the system from the images. i.e. classify the images as AD, MCI, and CN. Figure 4 shows the structural architecture of the Inception V3 model.

C. Metadata Analysis

The ADNI data website provides explanatory data on the MRI files, which are explored in the remainder of this section. This section analyses the demographics of the testing procedures using the metadata, to provide an insight into the data used to train the edge detection system.

i The subject ID of the test personnel.
ii The age at the time of the visit to the test site.
iii The gender of the subject.

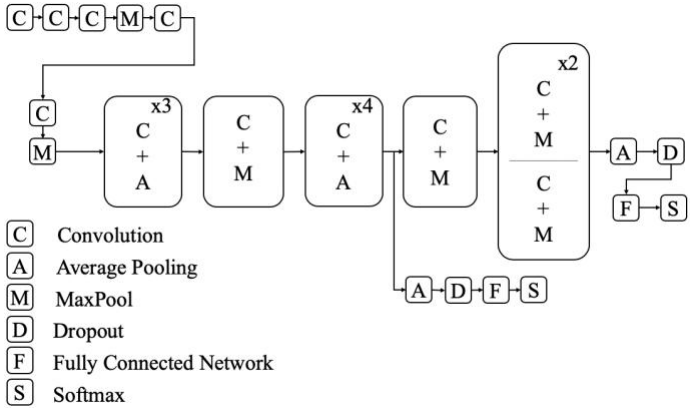

Fig. 4: Inception V3 Architecture

iv The classification group to which the test subject belongs.
v The number of times the subject has visited the ADNI site.
vi The types of pre-processing performed on the MRI data, before being converted to a NIfTI file. i.e. Gradwarp correction, B_1 correction and N3 sharpening.

818 subjects had undergone the test procedure, to produce a total of 9314 recordings of MRI study images. The distribution of the metadata is given in Table 1.

TABLE I: Data distribution of test subjects

Group	Sample Size	Age (years)	Gender [M/F]	Visit
CN	2896	76.8±5.2	1451/1451	3±2
MCI	4631	75.5±7.2	3048/1583	3±2
AD	1787	75.4±7.7	946/841	3±2

The correlation matrix amongst these features reveals the degree of impact on others.

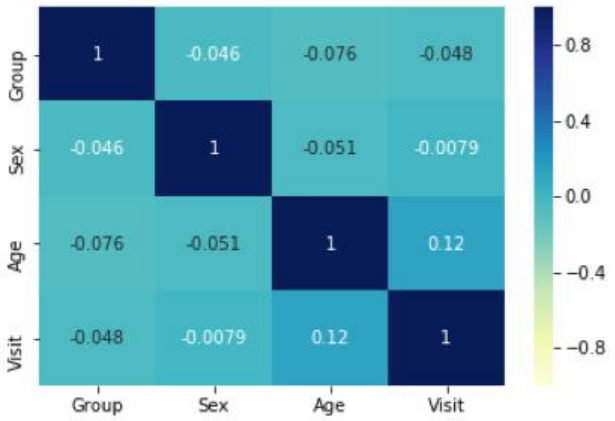

Fig. 5. Correlation matrix amongst meta data features

Form the correlation matrix, it is seen that the classification group exhibits the highest negative correlation with age. This shows that AD and MCI are detected for the subjects younger than that of CN subjects in the overall average in the MRI tests.

International Journal of Engineering Research & Technology (IJERT)
ISSN: 2278-0181
Vol. 9 Issue 10, October-2020

On the contrary, age is positively correlated with the Visit parameter. This shows that, as the age of the subject increased, the number of visits to the site to undergo the procedures also increased to obtain sustainable test results. The box plot distribution of data between group and age is given as in figure 6 shows that 50 percent of the subjects are between the ages of 70 and 81.

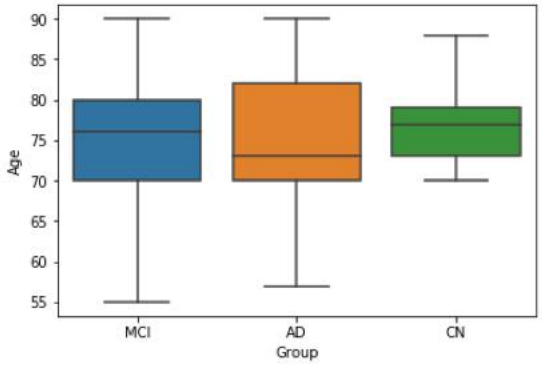

Fig. 6. Data distribution between Group and Age

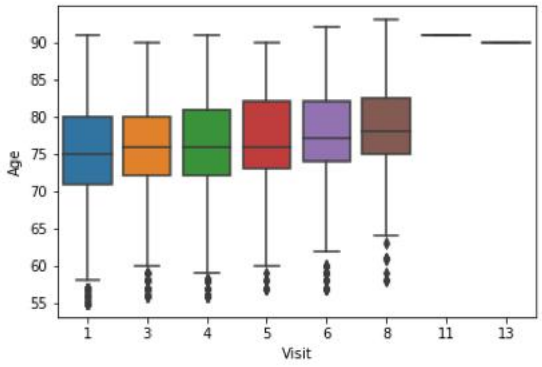

Fig. 7. Data distribution between Visit and Age

Figure 7 boxplot shows that the quantile age values increases with the increase in the number of visits to the test site. This shows that the visits to the testing facility were more frequent with the increase in age, exhibiting the fact that, the elderly were tested more.

D. Image Data Analysis

The data obtained from the ADNI website are of NIfTI format, that has been created by pre-processing the MRI data and converted to the format that retains the space orientation information of the MRI data. These files are converted to a desired image file format using the Nilearn python package version 0.5.0. Figure 8 shows the coronal cross-section of the MRI image, produced by Nilearn using a NIfTI file.

The images produced are of the dimensions 187 × 157 pixels. The Signal to Noise Ratio (SNR) is measured

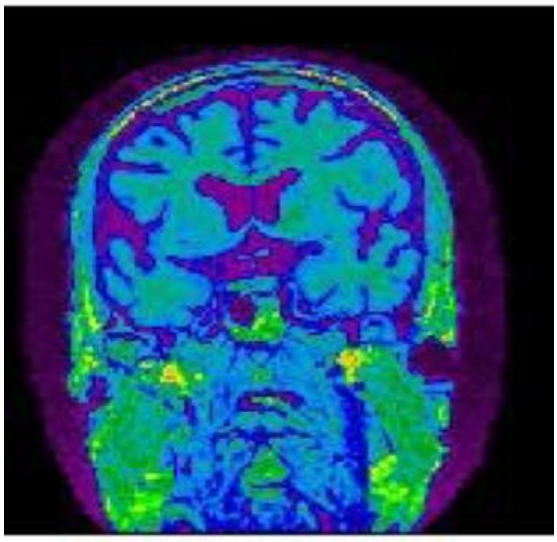

Fig. 8. Coronal cross-section of a subject's MRI

to calculate the dominance of noise in the image. The Equation. 1. shows the method equation used to obtain the SNR [8] value for this experiment.

$$SNR = {\mu_{signal}}/{\sigma_{signal}} \qquad (1)$$

Where μ is the average signal value from the image and σ is the standard deviation of the signal.

The average SNR of the images generated using the Nilearn package is approximately 0.889. This shows that the noise in the image is not insignificant.

The MRI images are also capable of revealing the visual difference between a CN brain and a brain with AD. The loss in brain matter resulting in a mass reduction in the hippocampus region and causing brain abnormality due to AD is shown in figure 9.

Figure 9 shows the regions of interest used, to detect the presence of AD. These are the regions used by the edge detection system to classify the MRI images by learning to differentiate the regions amongst the three groups.

E. Image Processing

From the previous section, it is seen that the images possess noise. The presence of noise over the signal power leads to poor detection of edges in the images by the system. Hence, the images must be pre-processed to reduce noise. The image is also normalized to maintain uniform intensity on all parts of the image.

*1) **Noise Reduction:*** The noise present in the images is reduced by smoothening the images. This is done by replacing the pixel intensities with the weighted average of the neighboring pixels. The weighted averages are calculated using Gaussian distribution $fg(x)$.

International Journal of Engineering Research & Technology (IJERT)
ISSN: 2278-0181
Vol. 9 Issue 10, October-2020

$$f_g(x) = \frac{1}{\sqrt{2\pi\sigma^2}} e^{-(x-\mu)^2/2\sigma^2} \qquad (2)$$

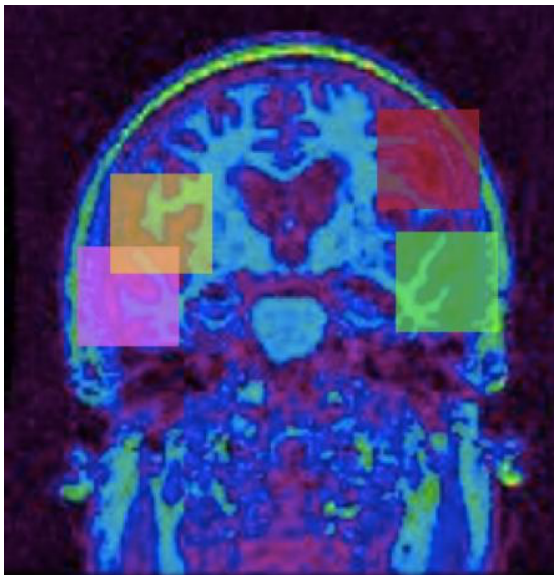

Fig. 9. MRI showing reduction in brain matter

Where μ is the average signal value from the image and σ is the standard deviation of the signal.

To achieve this operation, the Bilateral Filter is used. The Bilateral filter is superior to the conventional Gaussian filtering, as it can preserve the edges in the image while providing a similar level of noise reduction through the ability to control the intensity level of neighboring pixels. (3) denotes the bilateral filtering equation, referred from the research works of [9].

$$BF[I]_p = {}^{1}/_{W_p} \sum_{q \epsilon S} G_{\sigma_s}(||p-q||) G_{\sigma_r}(|I_p - I_q|) I_q \quad (3)$$

Where W_p denotes the Gaussian pixel weights

$$W_p = \sum_{q \epsilon S} G_{\sigma_s}(||p-q||) G_{\sigma_r}(|I_p - I_q|) I_q \qquad (4)$$

Where, G_{σ_s} is spatial Gaussian weighting, G_{σ_r} is the range Gaussian weighting, I_p is the intensity of pixel p and I_q is the intensity of pixel q.

Using the OpenCV package, version 4.2.0, the parameters sigma color and sigma space, of the inbuilt bilateral function are tested by iterating the pixel diameter through a range of values, to find the optimal image quality with defining edges of the image. Figure 10 shows the relation between the pixel diameter and Peak Signal to Noise Ratio (PSNR) for a different configuration of sigma color and sigma space.

From figure 10, it is evident that the PSNR peaks at pixel diameter between 2 and 10 and gradually decreases for all sigma color and sigma space values. By selecting the optimal sigma space and color configuration that produces the highest SNR and the highest PSNR, an image with clear edges and lesser noise is produced. Figures 11a and 11b show the difference between the original and the filtered image.

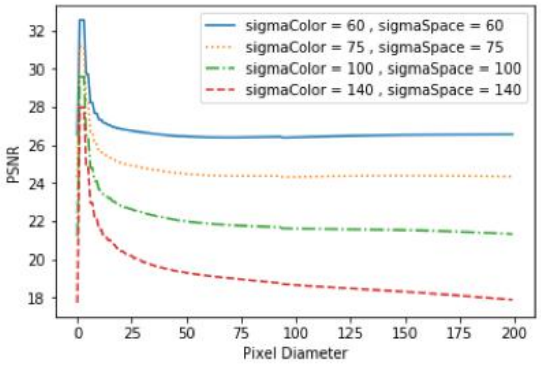

Fig. 10. Relation between pixel diameter and PSNR

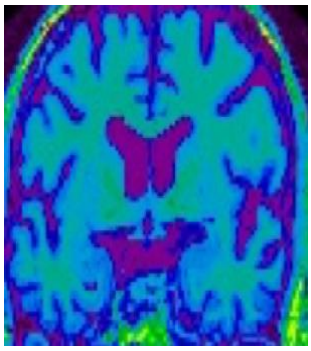

(a) Original MRI image

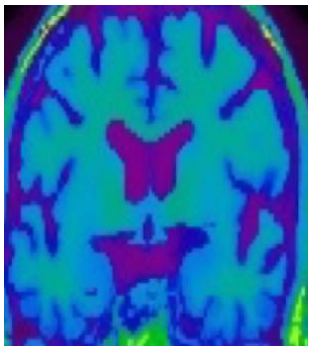

(b) Bilaterally filtered image

Fig. 11: Noise comparison between original Image and bilaterally filtered Image

2) ***Normalization****:* Normalization is a process done on the images, to homogenizes the pixel intensity. This provides an equal distribution of pixel strength. As a result, the edge detection system can detect the edges more efficiently for an image with more defining object boundaries. The normalization process utilizes the minimum and maximum intensities of the image. After normalization, the edges appear sharper than the bilateral filtered image.

The linear normalization performed for this experiment, follows the intensity range $I_N : \{X \subseteq R^n\} \rightarrow$

International Journal of Engineering Research & Technology (IJERT)
ISSN: 2278-0181
Vol. 9 Issue 10, October-2020

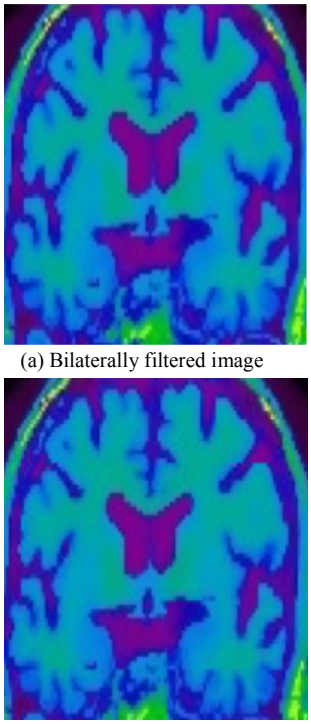

(a) Bilaterally filtered image

(b) Normalized image

Fig. 12: Image comparison between Bilaterally filtered image and Normalized image

$\{m_n, ..., M_n\}$. The equation followed for the normalization process is given as

$$I_N = (1 - m)\frac{M_n - m_n}{M - m} + m \qquad (5)$$

Where m is the minimum pixel intensity of the image, M is the maximum pixel intensity of the image, m_n is the new minimum intensity after normalization and M_n is the new maximum intensity after normalization.

F. Edge Detection System

A convolution neural network is used for the edge detection system, that has been trained to detect the edges of objects in the image and classify them based on the trained model. The system uses Inception V3 pre-trained weights to provide improved edge detection than a conventionally trained model. Figure 13 shows the edges detected by the Nilearn package. The edge detection system also utilizes a similar canny based algorithm to identify the edges.

The edge detection system is implemented using the TensorFlow framework, version r1.15. The system is tested on a computer machine having the following configuration. An HP Z4 G6 Tower workstation, having a 2.1 GHz octa-core Xeon Haswell – EP processor, that a 64 GB DDR4 DRAM utilizes, with an NVIDIA GeForce GeForce® GTX 1080 Ti consisting of 3584 CUDA cores, clocking at 1.5 GHz.

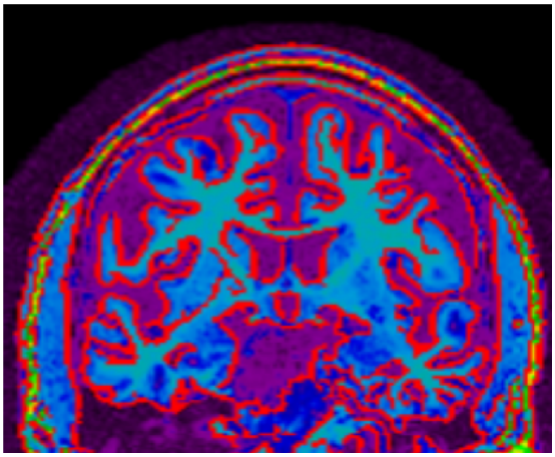

Fig. 13. Canny edges on MRI of a subject

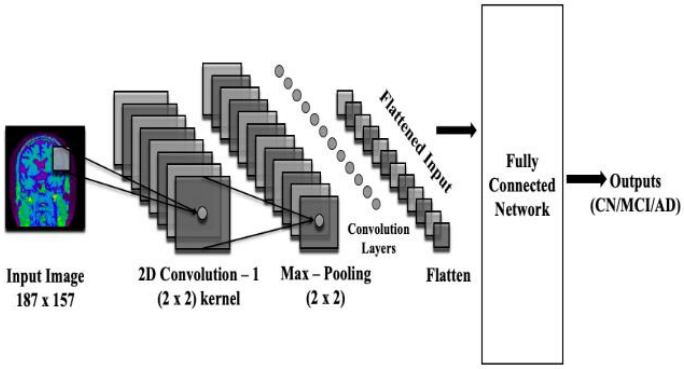

Fig. 14. Architecture of the proposed system

The weights of the convolution neural network are updated through back-propagation during the training process. The structure of the convolution network is given in figure 14.

The activation function used in the proposed model, for the input layers and the hidden layers is the Rectified Linear Unit (eqn. 6) (Fig. 15).

$$g(z) = \max(0, z) \qquad (6)$$

where z is the weighted summation of inputs. In the output layer, the SoftMax activation function (Fig. 15) is used, to categorize the images to their respective groups, based on the maximum probabilities predicted for each group.

G. Optimizer

The optimizer used for this experiment is Adaptive Delta Optimizer (ADADELTA). The optimizer performs optimally by reducing computational duration of the learning process significantly, with respect to other learning optimizers such as its predecessor, Adaptive Gradient. It also proves to be effective than Adam Optimizer. This is because of the exponential decaying average of the 2nd moment and the learning rate is adaptive. thereby, optimally improving the GPU usage and the model learning.

International Journal of Engineering Research & Technology (IJERT)
ISSN: 2278-0181
Vol. 9 Issue 10, October-2020

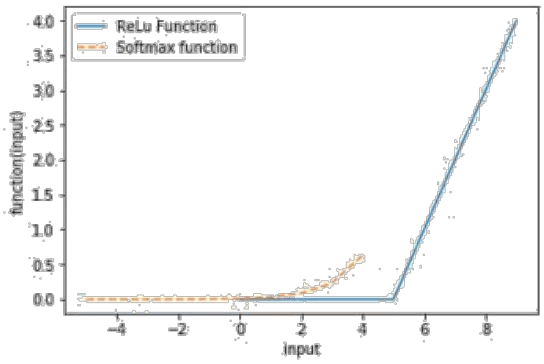

Fig. 15. ReLu and SoftMax activation Function

Equations 7-10 show the Adadelta optimizer states [10].

$$s_t = \rho s_{t-1} + (1-\rho) g_t^2 \quad (7)$$

$$g'_t = \sqrt{\frac{\Delta x_{t-1} + \varepsilon}{s_t + \varepsilon}} \odot g_t \quad (8)$$

$$x_t = x_{t-1} - g'_t \quad (9)$$

$$\Delta x_t = \rho \Delta x_{t-1} + (1-\rho) x_t^2 \quad (10)$$

Where, s_t= second moment of the gradient,
g_t = gradient,
g'_t = rescaled gradient,
x_t= leaky average of the second moment of the change of parameters in the model,
ρ = decay rate,
ε = fuzz factor.

Table 2. Shows the accuracy and loss results, comparing each of the optimizers tested in the experiment.

TABLE II: Validation results for different optimizers

Optimizer	Validation Acc. (%)	Validation Loss
Adadelta	80	1
Adagrad	64	1.07
Adam	54	1.04

H. Results

The experiment is conducted using a sample train dataset of size 6519 MRI images (70% of the dataset) to train the model for 10 epochs with a batch size of 32 samples. The Adadelta optimizer is applied in the system using the following configuration.

i Fuzz factor (ε) = $1e^{-1}$
ii decay rate (ρ) = 0

The results are validated with a 10-k fold validation that produces an average accuracy of 80%.

A sample test dataset (30% of the dataset), consisting of 2795 samples, is tested using the trained model. Figure 20

Fig. 16: Training loss of the system

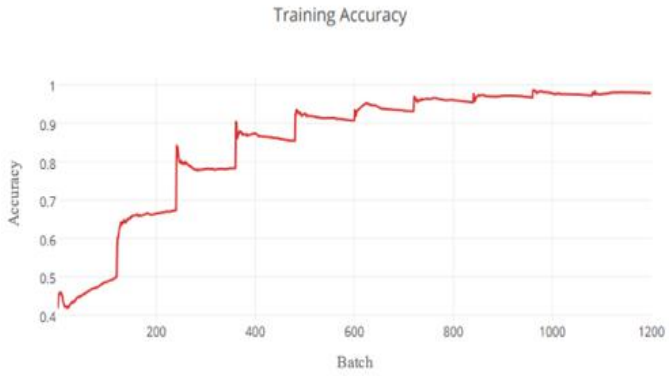

Fig. 17. Training accuracy of the system

shows the probability distribution of the predicted group for the test dataset.

Table 3. shows the confusion matrix result of the test dataset prediction.

The accuracy obtained for the test dataset, using the model is 82.89%. Table 4. shows the accuracy report for the test dataset.

A Support Vector Machine (SVM) classifier (linear kernel and $\gamma = 0.001, 0.0001$) and a Random Forest classifier with 100 estimators, are trained using the training dataset with 10-fold cross-validation and tested with the test

TABLE III: Confusion matrix for the test dataset results

Group	AD	MCI	CN
AD	447	87	6
MCI	22	1150	221
CN	127	15	720

TABLE IV: Accuracy report for the test dataset.

Group	Precision (%)	Recall (%)	f1-score (%)	Support (group count)
AD	75	83	79	540
MCI	92	83	87	1393
CN	76	84	80	862

International Journal of Engineering Research & Technology (IJERT)
ISSN: 2278-0181
Vol. 9 Issue 10, October-2020

Fig. 18. Validation loss of the system

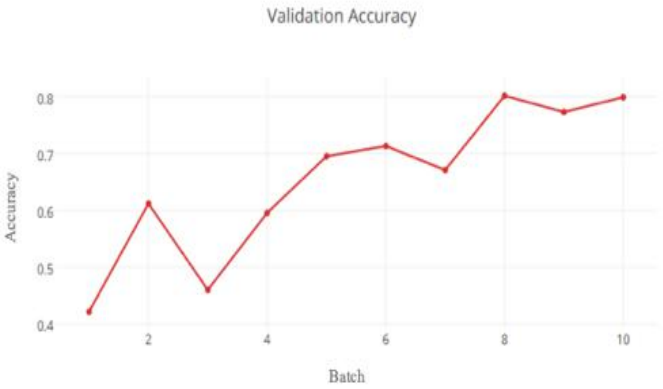

Fig. 19. Validation accuracy of the system

dataset. Table 5 shows the aggregated accuracies of all the prediction models proposed in this article.

The Inception V3 model predicts the classification groups of the test dataset of size 2795, in 322 seconds. Hence, the models can process an MRI image with a duration of 0.11s/sample. Although the SVM classifier and the Random Forest classifier can outperform the edge detection model, by predicting the classification groups for the test dataset in 0.079s/sample and 0.092s/sample

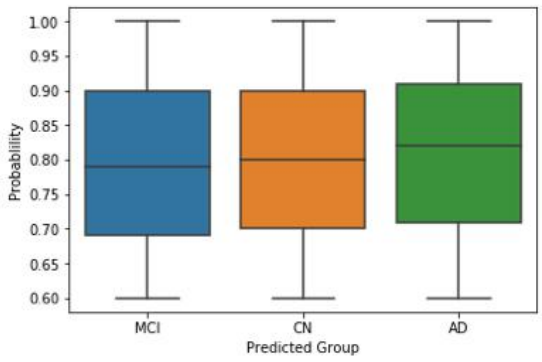

Fig. 20. Probability distribution of predicted group

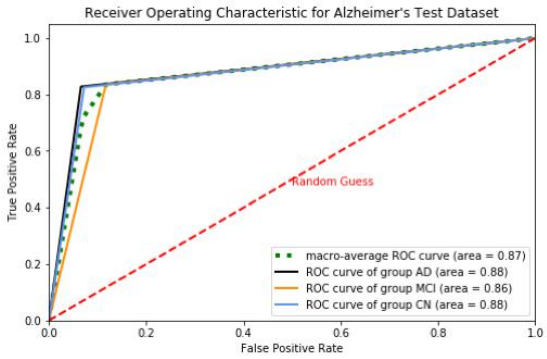

Fig. 21. AUC ROC of Test Dataset result

TABLE V: Accuracy report for the prediction models

Prediction Model	Accuracy (%)
Edge detection system	82.89
SVM	78.66
Edge detection system (without pre-processing)	76.00
Random Forest	75.52

respectively, the edge detection system can produce results with higher accuracy.

IV. Conclusion

An edge detecting system, that and classifies the brain MRI based on the abnormality observed the hippocampal region of the brain. Some of the conclusions derived from this experiment are listed below.

i The loss of brain matter registered in the MRI is utilized to train the model. thereby, detecting cognitive impairments.
ii The brain MRI shows a significant difference amongst the classification groups to be recognized by the system.
iii The accuracy of the correctly classified image is proportional to the quality of the image.
iv The edge detection system outperforms the SMV and the Random Forest classification algorithms.
v The edge detection system is efficient in processing the image within a short duration of time.

A. LIMITATIONS

Although the MRI scan can reveal the reduction in brain matter, which indicates possibilities of cognitive impairment, a physician must not conclude with the results provided by the automatic AD detection system. The patient must be subjected to further tests such as the Mini-mental state examination (MMSE), the Montreal Cognitive Assessment (MoCA) and the Self-Administered Gerocognitive Examination (SAGE).

B. FUTURE WORKS

This image detection system does not take into consideration the different types of brain matter, i.e. white

International Journal of Engineering Research & Technology (IJERT)
ISSN: 2278-0181
Vol. 9 Issue 10, October-2020

matter, gray matter while learning to classify the images. This system can be improved by enabling to differentiate between the types of brain matter and classify based on the significance of each brain matter on AD development.

ACKNOWLEDGMENT

Data used in the preparation of this article, are obtained from the Alzheimer's Disease Neuroimaging Initiative (ADNI) database (adni.loni.usc.edu). As such, the investigators within the ADNI contributed to the design and implementation of ADNI and/or provided data but did not participate in analysis or writing of this report. A complete listing of ADNI investigators can be found at: http://adni.loni.usc.edu/wp-content/uploads/how to apply/ADNI Acknowledgement List.pdf

REFERENCES

[1] John Elflein, Statista, Sep 24, 2019. Accessed on: November 24, 2019. [Online]. Available: www.statista.com/statistics/264951/number-of-people-with-dementia-from-2010-to-2050
[2] D. Marmanis et al. (2017). Classification with an edge: Improving semantic image segmentation with boundary detection. In: ISPRS Journal of Photogrammetry and Remote Sensing 135 (2018) pp 158–172.
[3] Christian Szegedy et al. (2015). Rethinking the Inception Architecture for Computer Vision. arXiv:1512.00567v3 [cs.CV] 11 Dec 2015.
[4] Alzheimer's Disease Neuroimaging Initiative. Accessed on: December 1, 2019. [Online]. Available: adni.loni.usc.edu/about/
[5] Alzheimer's Disease Neuroimaging Initiative. Accessed on: December 1, 2019. [Online]. Available: adni.loni.usc.edu/methods/mri-tool/mri-analysis/#mri-pre-processing-container
[6] Clifford R. Jack Jr. MD et al. (2008). The Alzheimer's disease neuroimaging initiative (ADNI): MRI methods. JOURNAL OF MAGNETIC RESONANCE IMAGING 27:685–691 (2008).
[7] Johannes Windschuh et al. (2015). Correction of B1-inhomogeneities for relaxation-compensated CEST imaging at 7T.
[8] ISO 12232, 2019 Photography — Digital still cameras — Determination of exposure index, ISO speed ratings, standard output sensitivity, and recommended exposure index.
[9] Sylvain Paris et al. (2009). Bilateral Filtering: Theory and Applications. Foundations and Trends in Computer Graphics and Vision Vol.4, No.1 (2008) 1–73
[10] 2009 S. Paris, P. Kornprobst, J. Tumblin, and F. Durand DOI: 10.1561/0600000020
[11] Aston Zhang et al. (2020). Dive into Deep Learning Release 0.7.1. Chapter 11, equation (11.9.1).
[12] John R et al. (2018). Detection of Alzheimer's Disease Using Fractional Edge Detection. Global J Technol Optim 9: 230. doi:10.4172/2229-8711.1000230
[13] D.P. Devanand et al. (2012). MRI hippocampal and entorhinal cortex mapping in predicting conversion to Alzheimer's disease. NeuroImage 60 (2012) 1622–1629.
[14] Andrea Chincarini et al. (2011). Local MRI analysis approach in the diagnosis of early and prodromal Alzheimer's disease. NeuroImage 58 (2011) 469–480.
[15] Elaheh Moradi et al. (2015). Machine learning framework for early MRI-based Alzheimer's conversion prediction in MCI subjects. NeuroImage 104 (2015) 398–412.
[16] L. Khedher et al. (2015) Early diagnosis of Alzheimer's disease based on partial least squares, principal component analysis, and support vector machine using segmented MRI images. Neurocomputing 151 (2015) 139–150.
[17] S. Li et al. (2007) Hippocampal Shape Analysis of Alzheimer Disease Based on Machine Learning Methods. AJNR Am J Neuroradiol 28:1339–45.
[18] O'BRIEN, J. T. (2007). Role of imaging techniques in the diagnosis of dementia. The British Journal of Radiology, 80(special_issue_2), S71–S77. doi:10.1259/bjr/33117326.
[19] Adrien Payan et al. (2015) Predicting Alzheimer's disease: a neuroimaging study with 3D convolutional neural networks. arXiv:1502.02506v1 [cs.CV] 9 Feb 2015.
[20] Batmanghelich, N. et al. (2009). A General and Unifying Framework for Feature Construction, in Image-Based Pattern Classification. Information Processing in Medical Imaging, 423–434. doi:10.1007/978-3-642-02498-6_35
[21] Bengio, Y. (2012). Practical Recommendations for Gradient-Based Training of Deep Architectures. Neural Networks: Tricks of the Trade, 437–478. doi:10.1007/978-3-642-35289-8_26
[22] Alex Krizhevsky et al. (2012). Imagenet classification with deep convolutional neural networks. In Advances in neural information processing systems, pages 1097–1105, 2012.
[23] Korolev, S. et al. (2017). Residual and plain convolutional neural networks for 3D brain MRI classification. 2017 IEEE 14th International Symposium on Biomedical Imaging (ISBI 2017). doi:10.1109/isbi.2017.7950647
[24] Saman Sarraf et al. (2015). Classification of Alzheimer's Disease Using fMRI Data and Deep Learning Convolutional Neural Networks. arXiv:1603.08631v1 [cs.CV] 29 Mar 2016.
[25] E. E. Tripoliti et al. (2008). "A supervised method to assist the diagnosis and classification of the status of alzheimer's disease using data from an fmri experiment," in Engineering in Medicine and Biology Society, 2008. EMBS 2008. 30th Annual International Conference of the IEEE, pp. 4419–4422, IEEE, 2008.
[26] Mahmood, R. et al. (2013). Automatic detection and classification of Alzheimer's Disease from MRI scans using principal component analysis and artificial neural networks. 2013 20th International Conference on Systems, Signals, and Image Processing (IWSSIP). doi:10.1109/iwssip.2013.6623471
[27] Kloppel, S. et al. (2008). Automatic classification of MR scans in Alzheimer's disease. Brain, 131(3), 681–689. doi:10.1093/brain/awm319
[28] Savio, A. et al. (2009). Classification Results of Artificial Neural Networks for Alzheimer's Disease Detection. Lecture Notes in Computer Science, 641–648. doi:10.1007/978-3-642-04394-9_78
[29] Huang, C. et al. (2008). Combining Voxel-based Morphometry with Artificial Neural Network Theory in the Application Research of Diagnosing Alzheimer's Disease. 2008 International Conference on BioMedical Engineering and Informatics. doi:10.1109/bmei.2008.245
[30] Davatzikos, C. et al. (2008). Detection of prodromal Alzheimer's disease via pattern classification of magnetic resonance imaging. Neurobiology of Aging, 29(4), 514–523. doi:10.1016/j.neurobiolaging.2006.11.010
[31] Deng X et al. (1999). Preliminary study on application of artificial neural network to the diagnosis of Alzheimer's disease with magnetic resonance imaging. Chinese Medical Journal. 1999 Mar;112(3):232-237.